NBS
Publi-
cations

NATIONAL BUREAU OF STANDARDS

NBS TECHNICAL NOTE 1152

U.S. DEPARTMENT OF COMMERCE / National Bureau of Standards

Mechanical Performance of Built-Up Roofing Membranes

NATIONAL BUREAU OF STANDARDS

The National Bureau of Standards[1] was established by an act of Congress on March 3, 1901. The Bureau's overall goal is to strengthen and advance the Nation's science and technology and facilitate their effective application for public benefit. To this end, the Bureau conducts research and provides: (1) a basis for the Nation's physical measurement system, (2) scientific and technological services for industry and government, (3) a technical basis for equity in trade, and (4) technical services to promote public safety. The Bureau's technical work is performed by the National Measurement Laboratory, the National Engineering Laboratory, and the Institute for Computer Sciences and Technology.

THE NATIONAL MEASUREMENT LABORATORY provides the national system of physical and chemical and materials measurement; coordinates the system with measurement systems of other nations and furnishes essential services leading to accurate and uniform physical and chemical measurement throughout the Nation's scientific community, industry, and commerce; conducts materials research leading to improved methods of measurement, standards, and data on the properties of materials needed by industry, commerce, educational institutions, and Government; provides advisory and research services to other Government agencies; develops, produces, and distributes Standard Reference Materials; and provides calibration services. The Laboratory consists of the following centers:

Absolute Physical Quantities[2] — Radiation Research — Thermodynamics and Molecular Science — Analytical Chemistry — Materials Science.

THE NATIONAL ENGINEERING LABORATORY provides technology and technical services to the public and private sectors to address national needs and to solve national problems; conducts research in engineering and applied science in support of these efforts; builds and maintains competence in the necessary disciplines required to carry out this research and technical service; develops engineering data and measurement capabilities; provides engineering measurement traceability services; develops test methods and proposes engineering standards and code changes; develops and proposes new engineering practices; and develops and improves mechanisms to transfer results of its research to the ultimate user. The Laboratory consists of the following centers:

Applied Mathematics — Electronics and Electrical Engineering[2] — Mechanical Engineering and Process Technology[2] — Building Technology — Fire Research — Consumer Product Technology — Field Methods.

THE INSTITUTE FOR COMPUTER SCIENCES AND TECHNOLOGY conducts research and provides scientific and technical services to aid Federal agencies in the selection, acquisition, application, and use of computer technology to improve effectiveness and economy in Government operations in accordance with Public Law 89-306 (40 U.S.C. 759), relevant Executive Orders, and other directives; carries out this mission by managing the Federal Information Processing Standards Program, developing Federal ADP standards guidelines, and managing Federal participation in ADP voluntary standardization activities; provides scientific and technological advisory services and assistance to Federal agencies; and provides the technical foundation for computer-related policies of the Federal Government. The Institute consists of the following centers:

Programming Science and Technology — Computer Systems Engineering.

[1]Headquarters and Laboratories at Gaithersburg, MD, unless otherwise noted;
mailing address Washington, DC 20234.
[2]Some divisions within the center are located at Boulder, CO 80303.

Mechanical Performance of Built-Up Roofing Membranes

James M. Pommersheim

Bucknell University
Lewisburg, PA

Robert G. Mathey

Center for Building Technology
National Engineering Laboratory
National Bureau of Standards
Washington, DC 20234

U.S. DEPARTMENT OF COMMERCE, Malcolm Baldrige, Secretary
NATIONAL BUREAU OF STANDARDS, Ernest Ambler, Director

Issued December 1981

National Bureau of Standards Technical Note 1152
Nat. Bur. Stand. (U.S.), Tech. Note 1152, 60 pages (Dec. 1981)
CODEN: NBTNAE

TABLE OF CONTENTS

LIST OF TABLES

LIST OF FIGURES

MECHANICAL PERFORMANCE OF BUILT-UP ROOFING MEMBRANES

James M. Pommersheim[1/]

Robert G. Mathey

ABSTRACT

For built-up roofing membranes with either linear or non-linear stress-strain behavior, fully bonded to an underlying deck or substrate which undergoes displacement, it is the equality of the complementary strain energy of the fabric or felt layer, with the strain energy of the bonding adhesive or bitumen layer, which governs both the conditions under which membrane integrity is lost and the mode of failure by either membrane splitting or adhesive disbonding. The testing criteria developed are applied to a sample case.

Key words: adhesive; bitumen; bonding; built-up roofing membrane; complementary strain energy; felt; non-linear; roofing membrane; splitting; strain energy; stress; substrate.

1. INTRODUCTION

A roofing membrane should be waterproof, and it should be able to sustain building movements. Unanticipated movements can lead to failure of the membrane. The mechanical function of a built-up roofing membrane

---

[1/] Professor of Chemical Engineering, Bucknell University, on assignment to NBS under provisions of the Intergovernmental Personnel Act.

is to prevent failure by effectively transferring shear stresses from one adjacent layer of the membrane to the next without loss in membrane integrity.

In this report, theory is developed and tested for roofing membrane strains and stresses which are induced by substrate movement. For simplicity, the roofing membrane is considered to consist of a single ply of roofing felt which is fully bonded with a bitumen (asphalt or coal tar pitch) layer to an underlying substrate. In practice, most bituminous built-up roofing membranes consist of asphalt saturated organic-felts and air-blown asphalt. Other materials used in roofing membranes are asphalt impregnated glass felts, asphalt saturated asbestos felts, coal tar pitch saturated organic felts, and coal tar pitch. The substrates over which membranes may be applied include insulation materials such as fiberboard, perlite board, fiberglass or foamed plastic, or, if no insulation is used, a roof decking material such as concrete, wood, or metal. In practice built-up roofing membranes consist of more than one ply. However, the mechanical performance of a single-ply membrane is not unlike that of a multi-ply or built-up roofing membrane [1].

When a roof is constructed using insulation, the separate pieces or sections (nominally, 2 or 3 x 4 ft (0.6 or 0.9 x 1.2 m)) are generally laid down in a staggered fashion upon the roof deck. The roofing membrane is then applied in shingle fashion over the insulation. Two to four-ply membranes consisting of alternating layers of fully bonded bitumen (asphalt or coal tar pitch) and felt are generally used.

Splitting of the membrane is one of the principal modes of failure of a built-up roof [1,2]. Loss of membrane integrity and penetration of water is the inevitable result. When splitting occurs it usually happens over the insulation joints where the membrane is subjected to the greatest amount of stress. In practice, staggering of the insulation boards helps to minimize the potential for lengthy splits in the roof membrane, as does placing the membrane with its strongest direction (the machine direction) perpendicular to the continuous joints in the insulation. Cullen and Boone [3] claimed that their own data, as well as that of Koike [2], supported the validity of Cullen's [4] original suggestions regarding the alteration of some conventional application techniques to reduce the incidence of splitting failures resulting from mechanically and thermally induced forces. Cullen's recommendations were:

(a) to place the insulation boards with the long dimension parallel to the short dimension of the roof,

(b) to orient the roofing felt parallel to the long dimension of the roof, and

(c) to use an adhesive (bitumen) of optimum strength to secure the membrane to the substrate.

Although such measures help to minimize membrane failure, they cannot prevent it when sufficiently large joint movements occur. Often these movements arise because of sudden temperature changes either inside or outside the building. Wetting and drying of some membranes will also induce stress in these membranes, as will wetting and drying of the underlying insulation or other substrate. It is the movement of the roofing membrane relative to the substrate which is important in determining if membrane failure may occur. Koike [2] found that membrane failure occurred in single-ply membranes for joint spacings or widths between 1.0 and 1.7 mm. Maximum movements of roof joints as high as 4 to 5 mm have been observed by Marijs and Bonafont [5] with a maximum movement rate of 0.3 mm/h. For safety they recommend that, over the lifetime of the membrane, a single layer of felt should not be fully bonded across a substrate joint if movement at the joint is likely to exceed 0.2 mm, and caution that overstressing or fatigue failure are likely even under summer conditions whenever joint movements exceed 1 mm.

A useful calculation to perform is to estimate the temperature difference, ΔT, between the substrate and the membrane needed to cause a joint movement of 0.2 mm. For example, consider a four-ply organic felt and asphalt roofing membrane fully bonded to an underlying substrate consisting of foam polyurethane rigid board. From 0° to 30°F (-18° to -1°C) Mathey and Cullen [6] report a coefficient of linear thermal expansion (α) for the membrane of 2.3×10^{-5} mm/mm/°C in the cross-machine or transverse direction and 5×10^{-6} mm/mm/°C in the machine or longitudinal direction, while in the same temperature range the insulation has an α value of 2.2×10^{-4} mm/mm/°C. For a typical roofing insulation board width, these values predict potential joint movements of 0.2 mm when the temperature change is about 1°C. Since temperature changes higher than this are often found in roofing insulation materials [7], this calculation points out the importance of proper roofing design in order to minimize temperature changes in roofing systems

Mathey and Cullen [6] have proposed the thermal shock factor (TSF) which is intended to provide a quantitative measure of the thermal-shock resistance of bituminous built-up roofing membranes

$$TSF = \frac{P}{M\ \alpha} \tag{1}$$

P is the tensile strength (ultimate or breaking load-force per unit width) of the membrane, M is the elastic modulus and α is the coefficient of linear thermal expansion.[1/] In their definition of the thermal shock factor, Mathey and Cullen [6] use a coefficient of linear thermal expansion based on values measured in the temperature range 0 to -30°F (-18 to -34°C).

The larger the magnitude of the thermal shock factor of a membrane the better able it is to withstand a combination of thermally and mechanically induced stresses. The concept of the thermal shock factor has proved useful as a means to assess the behavior of a wide variety of different types of roofing membranes [3]. Nevertheless, equation 1 is valid only for a membrane with linearly elastic (Hookian) stress-strain behavior.

In a built-up roofing membrane, the bottom ply of felt carries most of the load, and, in general, determines the resistance of the entire membrane to substrate movements [5]. The amount of the total load carried by the base felt will depend on the amount of bitumen flow which occurs initially during the loading period. If temperature and

---

[1/] A table of nomenclature is provided in Section 7 of this report.

strain are high then the amount of bitumen flow will be high, and the base felt will carry a larger proportion of the load [5]. In addition, the tensile strength of the membrane at higher temperatures will be lower.

As mentioned earlier, a single-ply system, such as that considered in this report, has a mechanical performance not unsimilar to a multi-ply system. For example, for linearly elastic materials, Bonafont [1] calculated that a two-ply membrane (consisting of a bottom bitumen layer, felt layer, second bitumen layer, and top felt) had only 12% more joint movement capability than a single-ply membrane (consisting of a bottom bitumen layer and a single top felt). If the bottom ply ruptures, the top ply has an ultimate movement capability which is then 41% greater. However, all the stress must now be carried by the top ply, and if it is weaker than the bottom ply, Bonafont [1] predicts that its failure will be entrained in the failure of the base ply. For safety he recommends that the stronger ply be placed on top, so that even if the base ply fails, the overall integrity of the roofing system will be maintained. With four plies the ultimate movement capability is increased by about a factor of two over that of a single ply system. As a rough rule, ultimate movement capacities for an N ply membrane are $\sqrt{N}$ times those of a single-ply system [1].[1/] This rule may be used to estimate movement capacities for non-linear membranes.

[1/] More extensive theory and discussion concerning the movement of multi-ply membranes caused by substrate joint movements have recently been presented in a paper by Koike *et al*. [9]. Treatment is restricted to membranes constructed of roofing materials having linearly elastic stress-strain characteristics.

Bonafont considers fatigue failure to be a more likely mode of mechanical failure than splitting due to overstressing [1,8]. Slip between fibers in the felt is irreversible so that cycling and repeated movements can cause failure sooner. Thus, failure by fatigue occurs at much lower values of joint spacing than does failure by overstressing. Bonafont found that if the felt is able to survive the first fatigue cycle it will survive a comparatively large number of identical cycles, since the greatest stress occurs in the first cycle. In his generalized development, Bonafont considered that the bitumen was a linear visco-elastic material. However, he did not consider the stiffening of the bitumen which often occurs as the membrane ages.

For proper roofing design, it is obvious that one must consider simultaneously many factors. Materials selection, heat transfer characteristics of the roofing system and substructure, cross-sections and thicknesses of the insulation and inter-ply bitumen layers, and the slope, weight, and kind of surface loading are factors which can all have a direct or indirect effect on joint movements and potential roof failure by membrane splitting or bitumen disbonding. In some instances a trade-off may be necessary between good insulatory properties which are favored by the use of thicker insulation, and small joint movements which are favored by the use of thinner insulation. Assuming that the insulation is well adhered to the roof deck, less restraint is offered to the change in length of the top of the thicker insulations by the deck when the roofing surface is subjected to temperature changes.

2. BACKGROUND

There are two basic related theories dealing with mechanical performance of roofing membranes subjected to stresses and strains induced by the movement of the underlying substructure; one developed by Koike [2], and one developed by Bonafont and co-workers [1,5,8].

Koike [2] derived a relation between joint movement in a substrate which is fully bonded to an elastic adhesive layer (generally a bitumen) and the resultant stresses and strains induced in the adhesive and membrane. He predicted the joint movement (or gap spacing) g needed to rupture a fully bonded fabric or felt layer having a tensile strength P and an elastic modulus M. The relation obtained was

$$g = 2\ P\ \left[\frac{h}{MG}\right]^{1/2} \qquad (2)$$

h is the thickness of the adhesive (bitumen) film between the substrate and the fabric and G is the shear modulus of the adhesive (bitumen). It is conventional in roofing system studies [1-6] to define both P and M based on the lateral felt width. G is based on the adhesive shear area.

Figure 1 depicts the physical situation. The system is shown both before and after substrate movement. Each substrate element moves horizontally a distance g away from the gap center line. Thus, the total gap width or spacing is 2g.

The most critical assumption involved in deriving Koike's relation is that both the fabric and the adhesive are linearly elastic or Hookian materials. In this case, a direct proportionality exists between stress

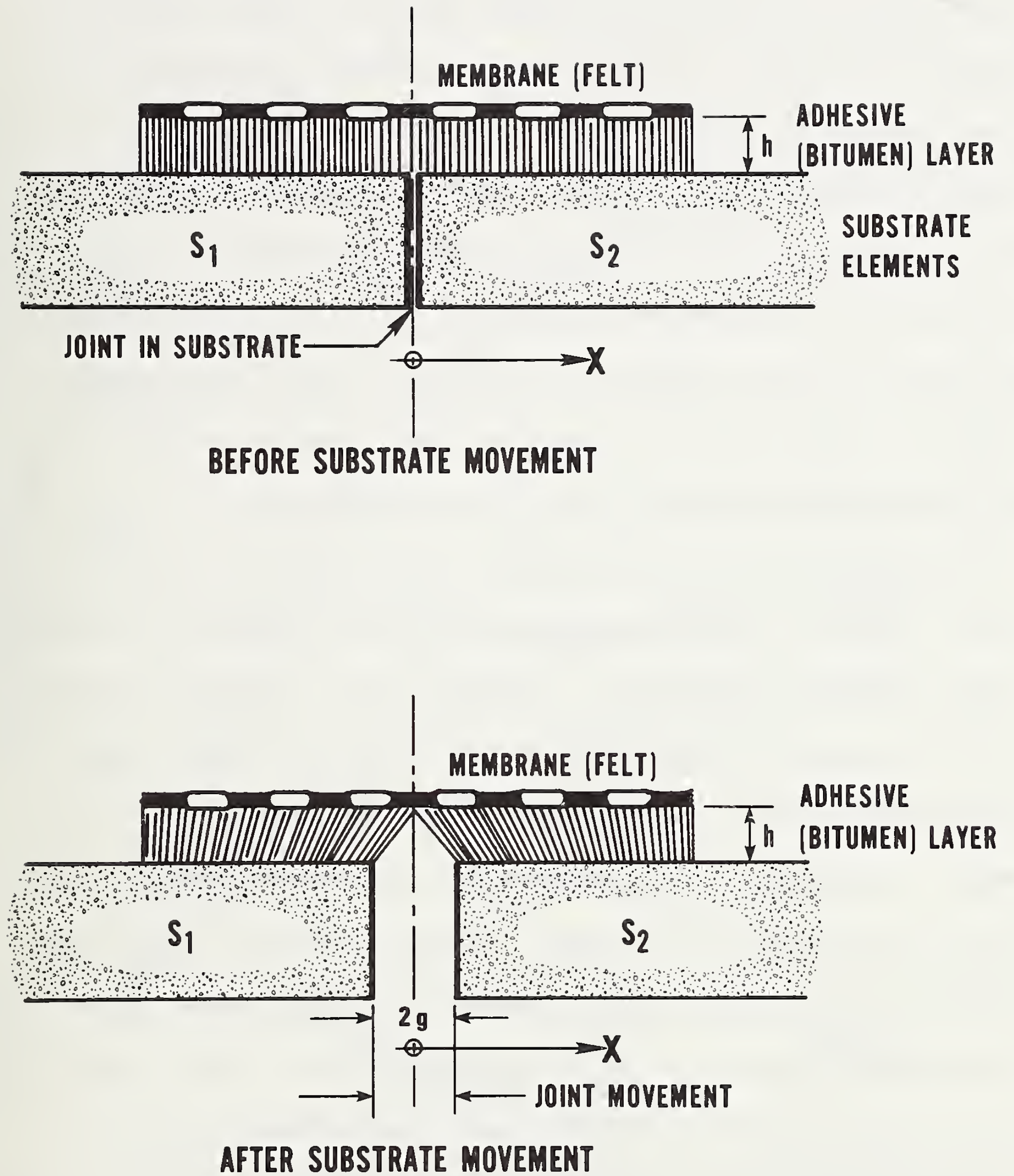

FIGURE 1. SCHEMATIC REPRESENTATION OF ROOFING MEMBRANE BEFORE AND AFTER SUBSTRATE MOVEMENT (1)

and strain, and the moduli M and G are presumed to be strictly constant. It is well known, however, that the moduli of roofing materials are not constant [1,10]. Marijs and Bonafont [5], for example, have found that a model which allows for both viscous and elastic properties, the so-called linear visco-elastic or Boltzmann model, is adequate for characterizing roofing systems. In fact, linear stress-strain diagrams for roofing materials seem to be the exception rather than the rule. Only at low temperatures (generally below -18°C (0°F)) do these materials show linearly elastic behavior, and then over only narrow ranges of stress application which are generally lower than those that cause splitting failure in actual built-up roofing systems.

The stress-strain data obtained by Koike [2] are distinctly non-linear. Figures 2 and 3 show stress-strain data collected by Koike [2] at three different temperatures. Figure 2 is for asphalt-saturated roofing felt (coated type), while figure 3 is for bonding bitumen (a blown-petroleum type). Both series of figures are definitely non-linear. In general, for the bitumen the curves bend upward, while for the felt the curves bend downward. As shown in figure 2, the non-linearity is more pronounced for the felt at higher temperatures, while for the bitumen (figure 3) it is more pronounced at lower temperatures. Figures 2 and 3 also show that at higher temperature the ultimate or breaking strength of both bitumen and felt is lower. These facts and the nature of the curves shown in figure 2 are also representative of those found for multi-ply built-up roofing membranes [5,9].

Thus, the non-linear response of the materials of construction of a built-up roof to imposed loads may be an important consideration in

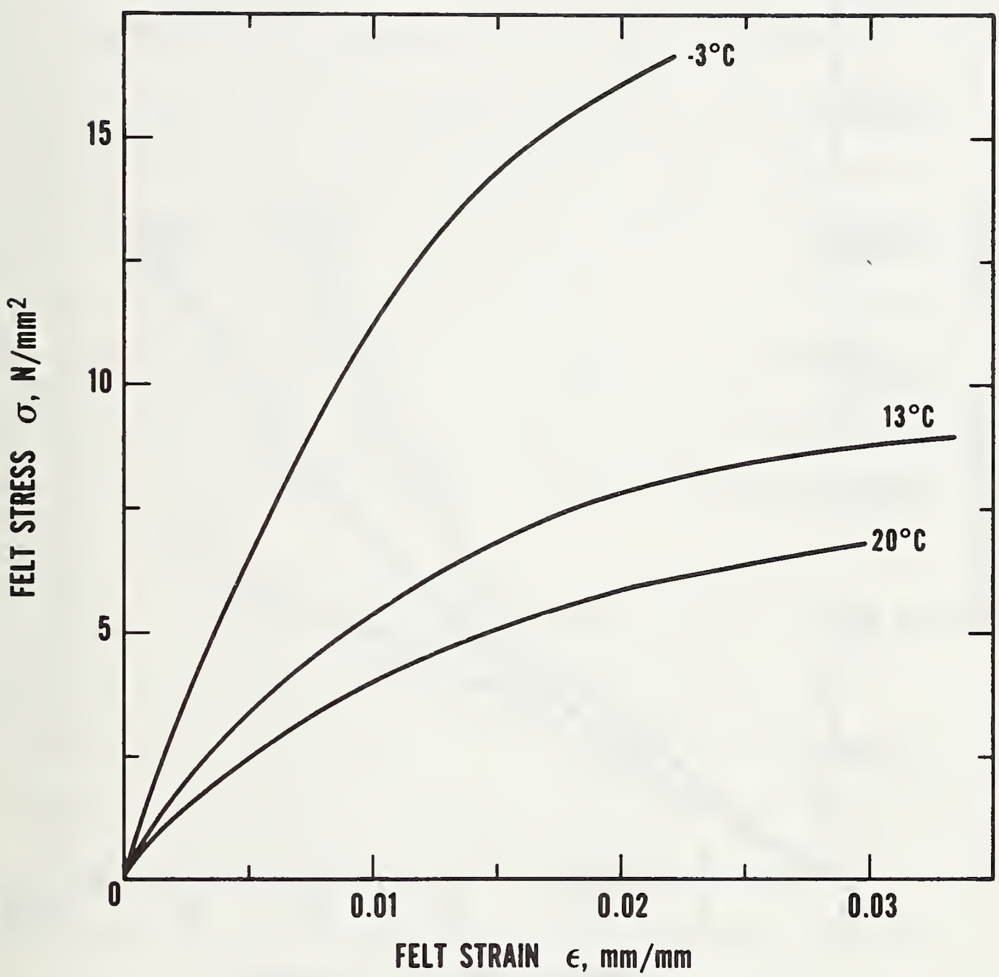

FIGURE 2. STRESS-STRAIN DIAGRAM FOR ROOFING FELT (2)

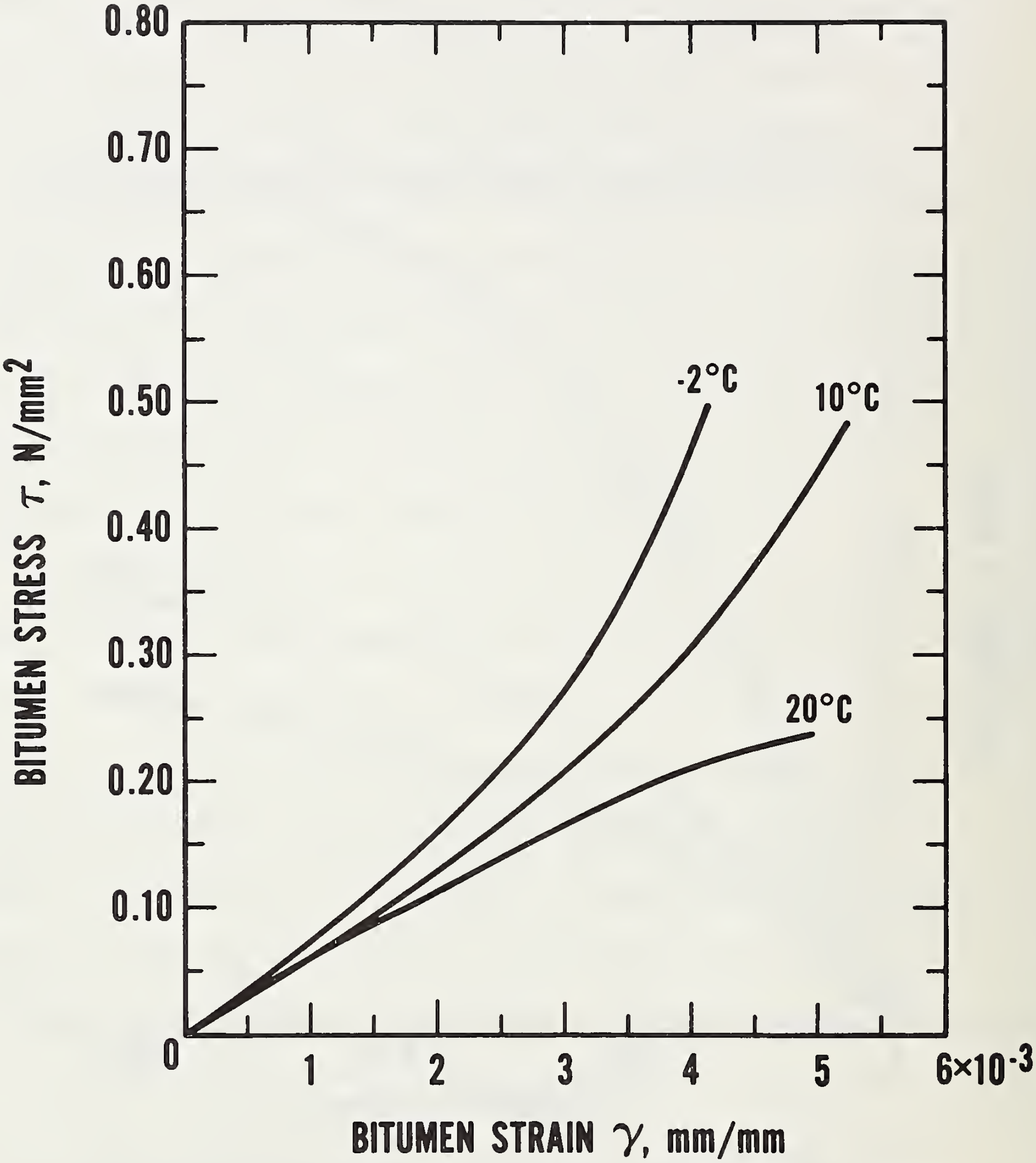

FIGURE 3. STRESS-STRAIN DIAGRAM FOR ROOFING BITUMEN(2)

their design and selection. Although Koike [2] realized that roofing materials are not linearly-elastic, he did not account in his analysis for the effects of the non-linearities. Koike obtained the value of M, the elastic modulus of the felt used in equation 1, by taking the slope of the stress-strain curve (figure 2) at the origin. Values of G, the shear modulus of the bitumen, he took equal to the slope of a line drawn from the origin to the ultimate or breaking stress of the bitumen. At the lowest temperature used (-3°C), where it was expected that the base felt would rupture, bitumen disbonding from the underlying mortar occurred instead. Koike attributed this to the fact that the bitumen shear tests were conducted with a stronger bond between the bitumen and the mortar than were the actual rupture tests. Thus, the bitumen separated from the mortar surface with a smaller shearing force than expected.

Koike [2] claimed that a rheological analysis of the problem of predicting gap widths from mechanical properties of roofing materials was impossible for non-linear or visco-elastic materials. Bonafont [1] was able to extend Koike's work to fabric or felts with non-linear and visco-elastic stress-strain behavior. Bonafont considered the rheological behavior of the bitumen to be that of an ideal Boltzmann-type (linear visco-elastic) body. In addition, he presented a more general theory for linearly elastic fabrics and adhesives, one which allows for the finite length of the substrate elements. The equation he developed for the joint movement is

$$g = \frac{2\ W\ P}{M[aW\ \coth(aW)-1]} \tag{3}$$

with

$$a^2 = \frac{G}{h\ M} \tag{4}$$

W is the half width of one substrate element. The bitumen is presumed to be fully bonded across two adjacent parallel substrate elements of total width 2W. Bonafont stated that equation 3 reduces to Koike's relation (equation 2) under the condition that (aW) >> 1.

In roofing practice this condition is the rule rather than the exception. Because of the fact that substrate element widths are much greater than bitumen film thicknesses, the dimensionless group (aW) will be much larger than unity. Under this condition equation 3 becomes

$$g = \frac{2\ W\ P}{M(aW\ -\ 1)} \tag{5}$$

Equation 5 further reduces to Koike's relation, equation 2, since under these conditions the quantity (aW - 1) can be approximated as aW. Koike's relation satisfactorily treats all two-ply membrane systems composed of materials with linear stress-strain behavior.

For non-linear membranes, Marjis and Bonafont [5] derived the following expression for the joint movement at which rupture should occur

$$g = 2\ \left[\frac{2hU}{G}\right]^{1/2} \tag{6}$$

U is the complementary strain energy of the felt, defined as the integral under its strain-stress diagram [11], that is,

$$U = 1/2 \int_{0}^{P} \varepsilon \, d \, \sigma \tag{7}$$

where ε is the strain and σ is the stress in the felt.

For a Hookian or linearly elastic felt, for which the stress is proportional to the strain, equation 7 reduces to

$$U = \frac{P^2}{2 M} \tag{8}$$

Substitution of equation 8 into equation 6 again yields Koike's relation, equation 2.

3. THEORETICAL DEVELOPMENT

3.1 Determination of Stress-Strain Relations for Felt and Bitumen

For materials with Hookian or linearly elastic stress-strain characteristics, the standard rate laws for the stresses in the felt and bitumen film layers, are, respectively

$$\sigma = M \, \varepsilon \tag{9}$$

$$\tau = G \, \gamma \tag{10}$$

τ is the stress in the bitumen (adhesive) and γ is the bitumen strain. By convention, τ is based on unit bitumen area. σ is based on unit felt width.

Before theory can be developed and applied to calculate joint movements for non-linear materials, it is necessary to find accurate constitutive relations for the stress-strain behavior of these materials.

The moduli M and G are constant only for a purely elastic membrane and film. But as was pointed out in the previous section, membranes are usually far from elastic, so that in general

$$\sigma = M(\varepsilon)\ \varepsilon \tag{11}$$

and

$$\tau = G(\gamma)\ \gamma \tag{12}$$

must be used to represent the shear stresses, in the membrane and film, respectively. The moduli in these equations are then the ratio of ordinate to abscissa of their respective stress-strain diagrams. They vary continuously with the strain level.

If experimental data are available, constitutive relations can be derived for the stresses and moduli. For the data of Koike (refer to figure 2), as well as data from NBS roofing membrane tests [6], the simplest formulas which were found to adequately characterize the stress-strain behavior of roofing felts had the form

$$\sigma = M_o\ \varepsilon\ e^{-\alpha\varepsilon} \tag{13}$$

Since $M = \sigma/\varepsilon$ it also follows that

$$M = M_o\, e^{-\alpha\varepsilon} \tag{14}$$

M_o and α are empirical constants. M_o is the zero-strain modulus for the roofing felt. Graphically, it is the slope of the stress-strain (σ,ε) diagram (figure 2) at the origin. The constant α is a measure of the deviation of the felt from linearly elastic behavior. Higher absolute values of α give larger deviations. For linearly-elastic fabrics or felts, $\alpha = 0$, and equations 13 and 14 reduce to the Hooke's law form, equation 9.

The constants M_o and α can be obtained from the linearizing plot of the logarithm of the ratio of stress to strain vs the strain. Thus, from equation 13

$$\log\left(\frac{\sigma}{\varepsilon}\right) = \log M_o - \frac{\alpha}{2.303}\,\varepsilon \tag{15}$$

The intercept of a plot of $\log(\sigma/\varepsilon)$ vs ε is equal to $\log M_o$ while the slope is given by $(-\alpha/2.303)$. Figure 4 shows the fit of equation 15 to data taken from figure 2 at temperatures of -3°C, 13°C, and 20°C. For each curve in figure 2 approximately 18 points were extracted and used in the data analysis. The lines shown were obtained by the method of least squares. Confidence bands $(\pm\, ts_r)$ are drawn about each line.

Table 1 summarizes the least squares values obtained for M_o and α at the three temperatures together with the correlation coefficients and error band $(\pm\, ts_r)$ of the linearizing plots, and the 95% confidence

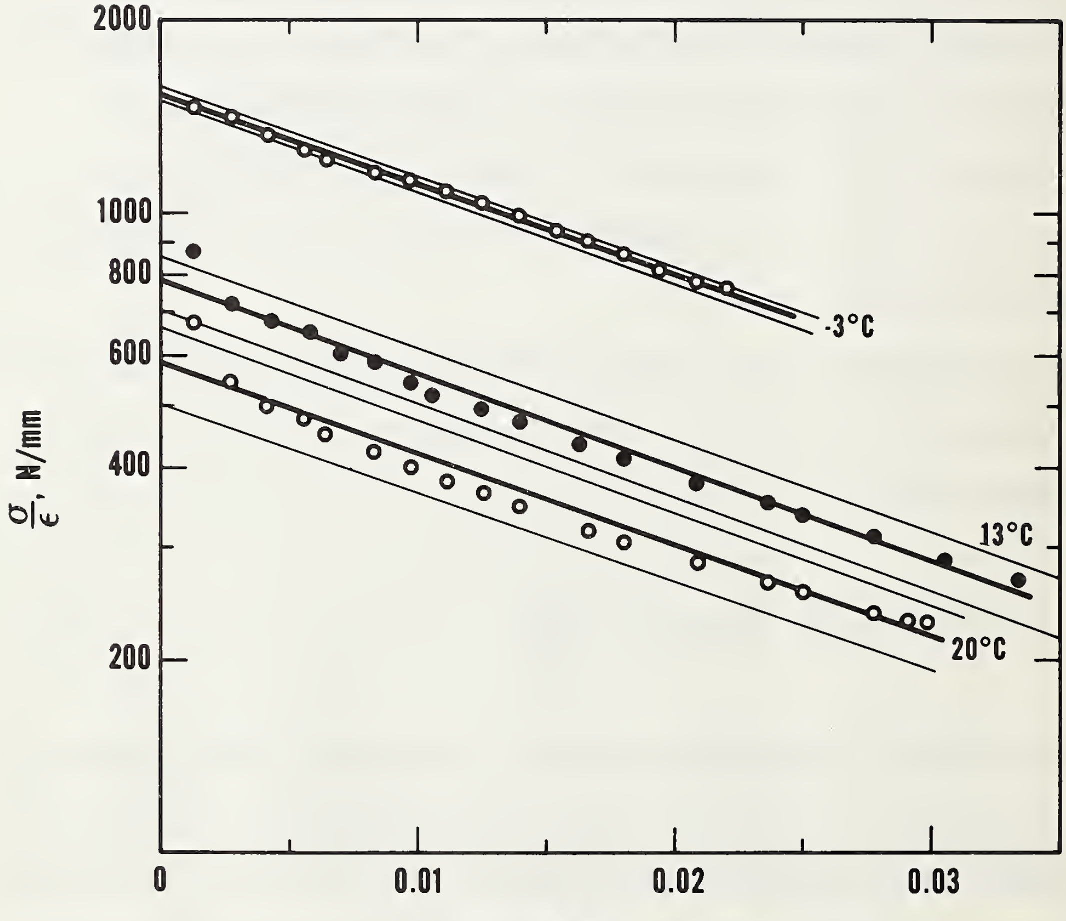

FIGURE 4. LOG σ / ϵ VERSUS ϵ (EQUATION 15)

Table 1[1/]

Analysis Using Equation 15 of Stress-Strain Data of Koike [2] for Roofing Felt

Symbol	Definition and Units	Temperature -3°C	13°C	20°C
r	correlation coefficient	0.998	0.990	0.982
$\pm ts_r$ [2/]	error band on best line (equation 15)	0.011	0.045	0.058
α	felt constant mm/mm	0.325	0.336	0.332
$\pm ts_\alpha$ [2/]	confidence band on α, mm/mm	0.004	0.011	0.015
M_o	felt zero-stress modulus, N/mm	15.41	7.82	5.82
$\pm ts_{M_o}$ [2/]	confidence band on M_o, N/mm	0.04	0.08	0.08
σ_m [3/]	predicted maximum stress, N/mm^2	17.46	8.58	6.44
ε_m [4/]	predicted strain at σ_m, mm/mm	3.08	2.98	3.01

1/ Based on 18 equal-spaced data points extracted from figure 2.
2/ Student's t values, 95% confidence bands.
3/ Calculated from 0.368 M_o/α.
4/ Calculated as $1/\alpha$.

bands on the values of α and M_o, ($\pm\ ts_\alpha$) and ($\pm\ ts_{M_o}$), respectively. Also included is the predicted maximum stress and the strain at this stress. The high values of the correlation coefficient r and the narrowness of the confidence bands indicate that equation 15 fits the data reasonably well.

The function $G(\gamma)$ can be evaluated by a similar procedure. The curves presented in figure 3 suggest that relations of the form

$$\tau = G_o \gamma e^{-\beta\gamma} \tag{16}$$

and, since $G = \tau/\gamma$

$$G = G_o e^{-\beta\gamma} \tag{17}$$

are adequate for characterizing data for the bitumen shear stress and bitumen shear moduli, respectively.

G_o and β are empirical constants, evaluable from experimental data. G_o is the zero-stress modulus for the roofing bitumen. Graphically, it is the slope of the stress-strain (τ,γ) diagram (figure 3) at the origin. The parameter β is a measure of the deviation of the bitumen from linearly elastic behavior. For linearly elastic bitumens, $\beta = 0$, and equations 16 and 17 reduce to the Hooke's law form, equation 10.

The linearized form of equation 16 is

$$\log (\tau/\gamma) = \log G_o - \frac{\beta}{2.303}\gamma \tag{18}$$

The intercept of a plot of log (τ/γ) vs γ is equal to log G_o while the slope is given by $(-\beta/2.303)$. Figure 5 shows the fit of equation 18 to data taken from figure 3, at temperatures of 20°C, 10°C, and -2°C. The lines shown were obtained by the method of least squares. Confidence bands $(\pm\ ts_r)$ are drawn about each line. Data points shown in figure 5 were extracted from figure 3. For each curve approximately 17 equally-spaced points were used. Table 2 summarizes the least squares values obtained for G_o and β at the three temperatures together with the correlation coefficients r of the linearizing plots, the 95% confidence bands on β and G_o, $(\pm\ ts_\beta)$ and $(\pm\ ts_{G_o})$, respectively, and the error band on the best line $(\pm\ ts_r)$. The fairly high values of r and the narrowness of the confidence bands on the slope and intercept indicate good agreement between the data and equation 18.

Note that both equations 13 and 16 contain two empirical constants (α, M_o; and β, G_o, respectively). As stated, both equations become constants at low stress levels, reducing to the Hooke's Law forms given by equations 9 and 10. This is in accord with both theoretical predictions and with most experimental data, where an initial linear portion of the stress-strain diagram is observed. In addition, equation 13 permits the existence of a maximum stress at the point where $\varepsilon = 1/\alpha$. The corresponding maximum stress is $[0.368\ M_o/\alpha]$. An analogous maximum bitumen shear stress of $0.368\ G_o/\beta$ at $\gamma = 1/\beta$ exists when β is positive.

Koike's data [2] yields negative β values for -2°C and 10°C and a positive β at 20°C. In his calculations, rather than allowing for any nonlinearities, he chose G to be the slope of a line from the origin of the τ - γ plot to the point where bitumen film failure occurs. For

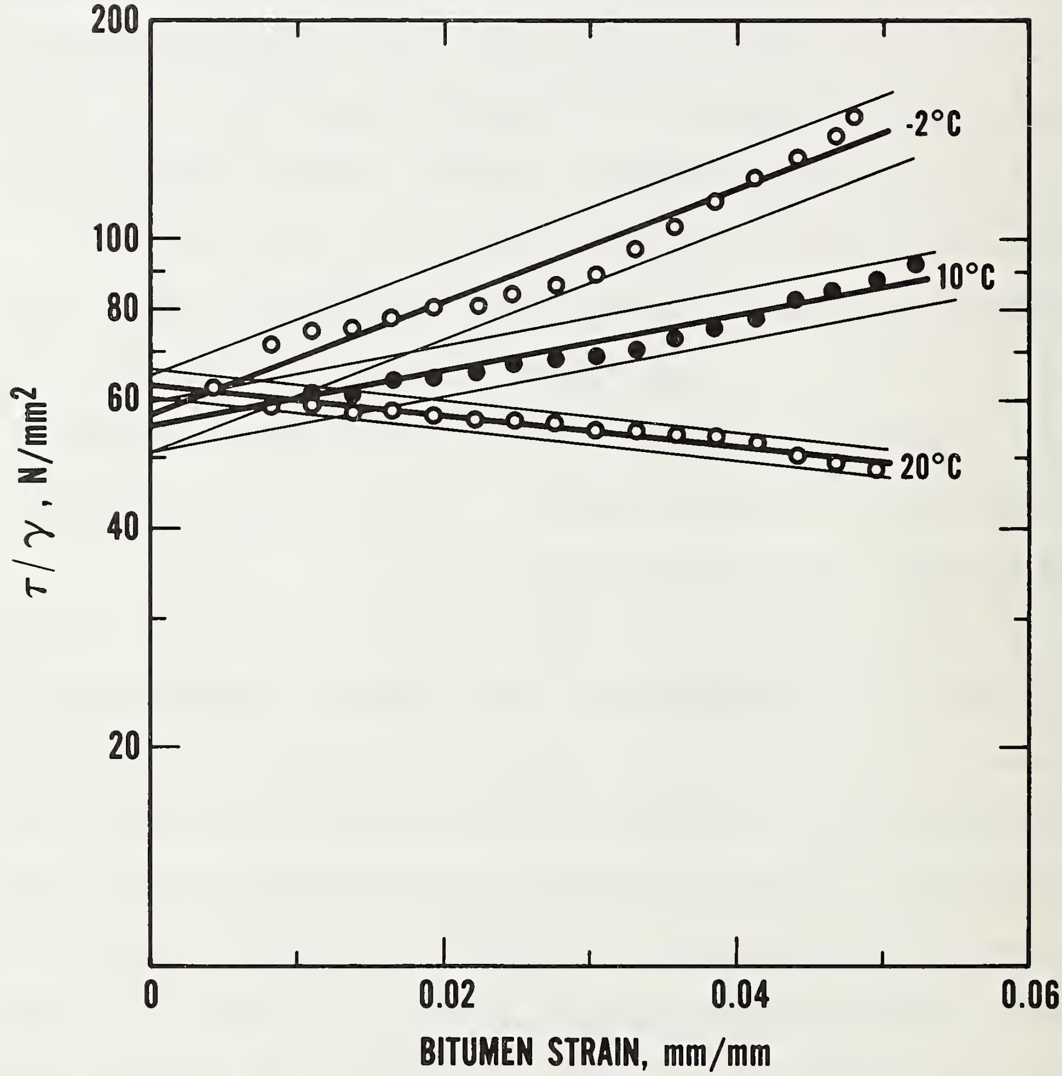

FIGURE 5. LOG τ/γ VERSUS γ (EQUATION 18)

Table 2[1]

Analysis Using Equation 18 of Stress-Strain Data of Koike [2] for Roofing Bitumen

Symbol	Definition and Units	Temperature -2°C	10°C	20°C
r	correlation coefficient	0.974	0.963	0.961
$\pm ts_r$[2]	error band on best line (equation 18)	0.054	0.035	0.018
β	bitumen constant, mm/mm	-1.786	-0.882	0.493
$\pm ts_\beta$[2]	confidence band on β, mm/mm	0.098	0.056	0.033
G_o	bitumen zero-stress modulus, N/mm^2	0.571	0.550	0.632
$\pm ts_{G_o}$[2]	confidence band on G_o, N/mm^2	0.008	0.004	0.003

1/ Based on 17 equal-spaced data points extracted from figure 3.

2/ Student's t values, 95% confidence bands.

bitumens having negative values of β this predicts joint movements for rupture which are less than the actual movement.

3.2 Mathematical Models for the Mechanical Performance of Roofing Membranes

In this section, theory is developed for roofing membrane strains and stresses induced by substrate movement. The prediction of these stresses and strains is important since they can lead to rupture or splitting of the membrane with resultant penetration of water, and possible subsequent slippage of the membrane. Movement of substrate joints can also cause shear failure by disbonding of bitumen from the underlying substrate. This begins at the location of the joint (see figure 6). The potential is then present for the bitumen to peel from the substrate surface. Peeling is promoted by increased air and water vapor pressure which develops at the disbonded joint between the membrane and substrate due to temperature and humidity changes within the roofing system. Peeling can lead eventually to the formation of ridge blisters which have been observed to develop over insulation joints.

Consider the roofing section depicted in figure 6. A bitumen coated felt is presumed to be fully bonded to an underlying substrate. The substrate is generally some type of roofing insulation or roof deck material. External forces such as those induced by temperature changes or shrinkage can cause fissures in the bitumen bonding layer and gaps to develop or widen between adjoining insulation boards or substrate elements. Strains are then transmitted to the overlying membrane. These in turn give rise to membrane stresses.

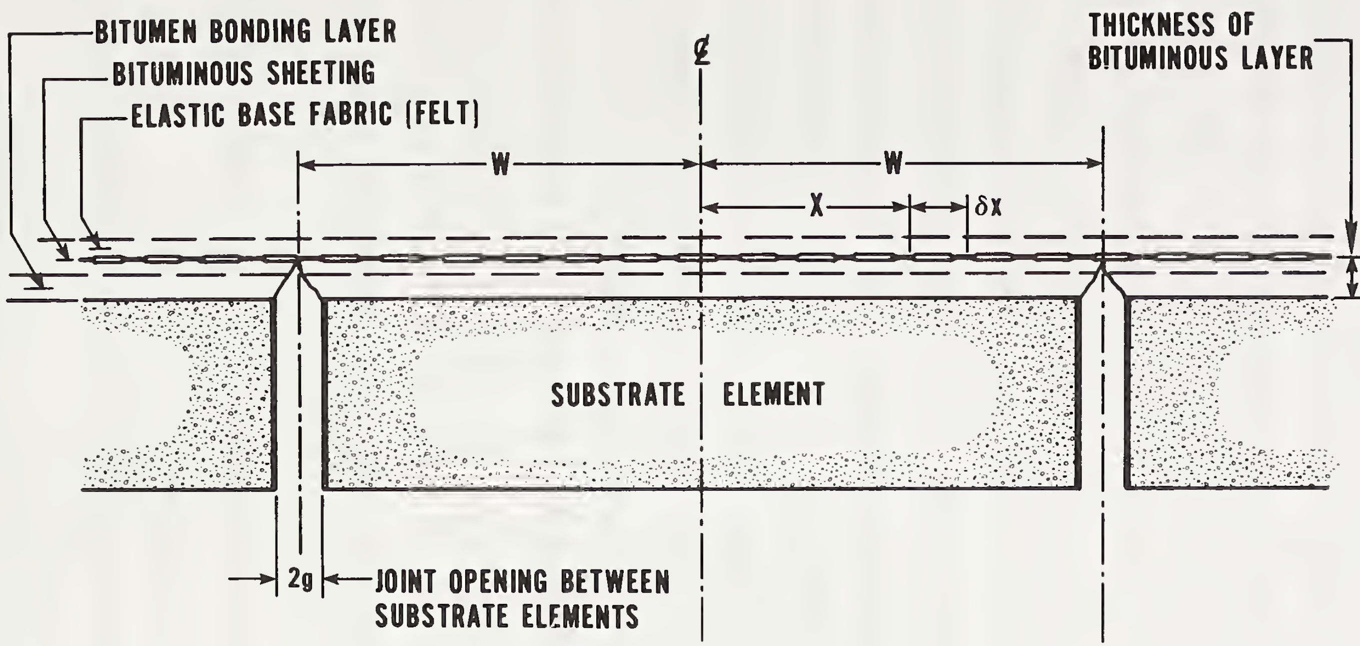

FIGURE 6. CROSS-SECTION OF ROOFING MEMBRANE AND SUBSTRATE (1)

Expressions are derived here for the joint movements which will cause either splitting of the felt layer or the disbonding of the bitumen layer from the substrate. The derivation is a generalization of the original linear theory of Koike [2] and is also related to the non-linear theory presented by Marijs and Bonafont [5]. However, it differs fundamentally from the theory of these latter authors in that it applies to both bitumens and felts having non-linear stress-strain behavior rather than to just felts alone having non-linear behavior.

The theory is based on mechanical force balances made on the membrane elements (bitumen and roofing felt) covering one idealized substrate element (insulation board), located somewhere in the middle of the roof (refer to figure 6). The prediction of the movement of the substrate itself is not considered in this report but is taken as known a priori. In general, such movements are caused by temperature differences within the insulation in a direction perpendicular to the roof deck (along the centerline in figure 6). Such temperature differences can be quite high, especially for today's well-insulated roofs. Calculations based on the heat-transfer model for roofing systems developed by Rossiter and Mathey [7] showed that temperature drops as high as 72°F (40°C) could occur across an insulation element on a hot, sunny day. For mechanically unconstrained elements, this could cause potential substrate movements as high as 0.4 in (10 mm).

The basic assumptions involved in the derivation of expressions for the joint movements include:

1. strains and strain rates are small and equal at every adjacent position in the bitumen and felt,
2. the membrane has low Poisson's ratio so that dominant stresses are only in the direction of the substrate movement,
3. joint movements are produced by the translation of one substrate element relative to another, rather than by the deformation of the elements themselves,
4. joint movement is small compared to both the length of the substrate element and to its width.

The first assumption comes from the fact that there is no relative movement between the felt and the bitumen, while the second and third, which are also true, imply that the problem can be treated mathematically using a single dimension. The last assumption is true in practice and also finds use in simplifying the mathematics.

The derivation which follows also presumes that the properties of the materials do not change with time. In practice this assumption may not be true, especially for new roofs where rapid bitumen aging may occur.

The shear stress in the bitumen film is given by

$$\tau = d\sigma/dx \qquad (19)$$

where, in general

x is the coordinate in the direction of the membrane displacement, measured from the center of the fissure or gap (figure 6),
$\tau(x)$ is the shear stress in the bitumen or adhesive film,
$\sigma(x)$ is the stress in the felt or fabric.

This equation is readily obtained from an x-direction force balance on a thin element of the film of volume $\Delta V = h\ B\ \Delta x$, where Δx is the length of the element, h is the thickness of the film between the substrate and the felt, and B is the width of the membrane (into the diagram in figure 6).

Membrane strain ε and substrate strain ζ are defined, respectively, by

$$\varepsilon = \frac{du}{dx} \tag{20}$$

and

$$\zeta = \frac{dv}{dx} \tag{21}$$

u(x) is the membrane displacement and v(x) is the substrate displacement. Both u and v are measured relative to the center of the gap (x = 0).

The movement of the film is defined in terms of the separate movements of the membrane and substrate by $\gamma(x)$, the shear deformation of the bitumen film

$$\gamma(x) = \frac{u(x) - v(x)}{h} \tag{22}$$

Combining equations 12 and 19

$$\frac{d\sigma}{dx} = G(\gamma)\ \gamma \tag{23}$$

Differentiating equation 23, using equation 22

$$h \frac{d^2\sigma}{dx^2} = [G + \gamma \frac{dG}{d\gamma}][\frac{du}{dx} - \frac{dv}{dx}] \tag{24}$$

or

$$h \frac{d^2\sigma}{dx^2} = \frac{d\tau}{d\gamma} [\varepsilon - \zeta] \tag{25}$$

Equation 25 follows from the strain definitions given by equations 20 and 21, and from equation 12.

Equation 25 is a non-linear equation of the second order. As such it needs two boundary conditions. These are given by

$$(\frac{d\sigma}{dx})_{x=0} = \frac{G(0)}{h} \frac{g}{2} \tag{26}$$

and

$$(\frac{d\sigma}{dx})_{x=W} = 0 \tag{27}$$

where G(0) is the value of G at x = 0. The first condition, equation 26, follows since there is no membrane displacement g at the center of the joint. The second condition, equation 27, is the result of the fact that x = W is a plane of system symmetry, and thus a line of zero bitumen shear stress.

The complementary strain energy U is defined by [11]

$$\frac{dU}{d\sigma} \equiv \varepsilon \tag{28}$$

U does not have the obvious physical meaning that the regular strain energy does, but is a useful mathematical construct for solving stress-strain problems involving non-linear materials or structures situations. Note that equation 7 is the integral of equation 28.

Introducing equation 28 into equation 25 and rearranging

$$h \frac{d^2\sigma}{dx^2} = \frac{d\tau}{d\gamma}\frac{dU}{d\sigma} - \frac{d\tau}{d\gamma}\zeta \tag{29}$$

Substituting equation 19 into equation 29, using the fact that

$$\frac{d^2\sigma}{dx^2} = \frac{d\tau}{dx} = \tau \frac{d\tau}{d\sigma} \tag{30}$$

gives

$$h\tau \frac{d\tau}{d\sigma} = \frac{d\tau}{d\gamma}\frac{dU}{d\sigma} - \frac{d\tau}{d\gamma}\zeta \tag{31}$$

Dividing through by $d\tau/d\gamma$ and using the fact that the displacement ζ is

$$\zeta = \frac{-g}{2W} \tag{32}$$

gives

$$h\tau \frac{d\gamma}{d\sigma} = \frac{dU}{d\sigma} + \frac{g}{2W} \tag{33}$$

Multiplying by $d\sigma$ gives an exact equation which on integration becomes

$$h \int_0^{\gamma} \tau \, d\gamma = U + \frac{g}{2W} \sigma + C_1 \tag{34}$$

Equation 34 is expressed in terms of the strain energy for the bitumen film, $\int \tau \, d\gamma$, the complementary strain energy for the felt U and the membrane stress σ. It must be true at each and every position x within the structure. In particular, at positions far from the joint the strain energies and stress levels will be small. This implies that the constant C_1 may be taken equal to zero so that equation 34 becomes

$$h \int_0^{\gamma} \tau \, d\gamma = U + \frac{g}{2W} \sigma \tag{35}$$

When the gap spacing g is much less than the membrane width W, the last term in equation 35 can be dropped. As discussed previously this is a reasonable assumption for all practical situations of interest. Thus

$$h \int_0^{\gamma(0) = \frac{g}{2h}} \tau \, d\gamma = \int_0^{\sigma(0)} \varepsilon \, d\sigma \qquad (36)$$

Equation 36 is a major result. It shows the equality of the product of the bitumen film thickness times the strain energy for bitumen shear with the complementary strain energy for felt or fabric shear. Since the greatest stresses occur above the joints (at $x = 0$) this equation is of greatest applicability there. This is shown in equation 36 by the use of the integration limits $\gamma(0)$ and $\sigma(0)$ which represent the bitumen strain and membrane stress, respectively, at the joint. The corresponding maximum bitumen shear stress at the joint is

$$\tau(0) = \frac{G(0)\ g}{2h} \qquad (37)$$

Equation 36 can be used whenever separate stress-strain data for the bitumen and the felt are available. The gap spacing g that will cause rupture of the felt is the one which would first give rise to the ultimate stress. Therefore, equation 36 can be solved graphically, or analytically if equations are available, to find the value of g which will first cause stress $\sigma(0)$ corresponding to P. Since equation 36 can be used to predict the incidence of membrane failure, it can be considered to be a general criterion for membrane failure.

In some cases the bitumen itself will not be able to transfer stress $\tau(0)$ corresponding to P. An ultimate shear strength $\bar{\tau}$ is reached which destroys the ability of the bitumen film to transfer shear stresses. $\bar{\tau}$ will generally be the lesser of (a) the shear required to break the bond at the interfaces between dissimilar materials, or (b) the shear required to rupture the adhesive itself.

In both cases the integrity of the fabric will be maintained at the expense of the adhesive. Bonafont [1] maintains that an artificial slip layer will be formed which will be able to subsequently absorb large substrate movements. This may be true, but it also appears to be a potential source of formation of ridge blisters in built-up roofs. This occurs because in the evening warm moisture laden air from the sides or below enters the peeled joint. Later the moisture condenses out as the roof cools. During the daytime when the roof is warm this moisture vaporizes and the pressure within the peeled joint rises, causing more peeling. Over time this day-to-day cycling action causes a ridge blister to develop as the peeling joint propagates the weakest direction, which is down the joint. Eventually the blister may enlarge to the point where the overlying fabric is stretched to its yield point and splitting occurs.

4. RESULTS AND DISCUSSION

In this section the theory derived for the mechanical performance of roofing membranes is applied to the constitutive stress-strain relations developed in the previous section. Results are discussed in terms of the mechanical conditions causing membrane failure and the mode of failure. Methods are presented for analyzing data to determine the incidence and mode of membrane failure. Comparisons are made with the results of Koike [2] for linearly elastic roofing materials.

It is easy to understand whether the strength of the felt (P) or the strength of the bitumen ($\overline{\tau}$) controls failure. The stronger material is whichever one has the greater strain energy as determined by the integrals in equation 36.

Quantitative predictions of the incidence and mode of failure can be obtained. Substituting equations 13 and 16 into equation 36, and integrating

$$\frac{hG_o}{\beta^2}\left[1 - \left(\frac{\beta g}{2h} + 1\right) \exp \frac{-\beta g}{2h}\right] =$$

$$\frac{M_o}{\alpha^2}\left[e^{-\alpha\varepsilon}\left(\alpha^2\varepsilon^2 + \alpha\varepsilon + 1\right) - 1\right] \tag{38}$$

Equation 38 is the criterion for membrane failure. It can be considered to be the working form of equation 36. The term before the equals sign in the equation represents the bitumen strain energy-film thickness product, while the term after the equals sign of equation 38 represents the complementary strain energy for the felt (U). Of course the validity of the equation is conditional on the applicability of the constitutive stress-strain laws (equations 13 and 16) to the data being considered.

All terms in equation 38 are evaluated at x = 0, where the greatest stresses act. If felt tensile strength P controls failure, equation 38 can be solved for the critical spacing g needed for rupture. The strain ε is replaced by the ultimate strain ε_p corresponding to P on the stress-strain diagram. If the bitumen film yield strength $\bar{\tau}$ controls failure the g calculated from

$$g = 2h\,\bar{\gamma} \tag{39}$$

will be less than that calculated from equation 38. $\bar{\gamma}$ is the bitumen shear strain corresponding to the stress $\bar{\tau}$. Use of this value of g will allow calculation of the felt strain from equation 38 and the felt stress from equation 21. This calculation is of importance for determining the residual stress still present in the felt. At higher stress levels felts having positive values of α can show two different strains (ε) at the same stress. This is because they may not rupture at the point of greatest stress.

For materials with linear stress-strain diagrams the solution is similar. Substituting equations 9 and 10 into equation 36, integrating and solving for the gap spacing g needed for rupture, yields Koike's relation, equation 2, which is valid for linearly elastic materials only. As mentioned in the previous section, Bonafont [1] developed a more general theory for membranes with linear stress-strain behavior, a theory which reduces to Koike's relation for small h/W. Since h/W is small in all roofing applications of interest, Koike's relation is valid as long as the membrane materials are linearly elastic.

In some cases the felt may be linearly-elastic while the bitumen remains non-linear. For this case $\alpha = 0$, $M_o = M$, and equation 38 reduces to (in the limit)

$$P^2 = 2hMG_o \left[1 - \left(\frac{\beta g}{2h} + 1\right) \exp \frac{-\beta g}{2h}\right] \tag{40}$$

It is also possible that the felt has non-linear stress-strain behavior, but the bitumen is a linearly elastic material. For this case $\beta = 0$, $G_o = G$, and equation 38 reduces to (in the limit)

$$g^2 = \frac{8hM_o}{G\,\alpha^2} \left[e^{-\alpha\varepsilon_p}(\alpha^2\varepsilon_p^2 + \alpha\,\varepsilon_p + 1) - 1\right] \tag{41}$$

For given mechanical properties of the bitumen and felt and a specified bitumen film thickness, equations 40 and 41 may be used to calculate the gap spacing g which governs failure of the roofing membrane by rupture of the felt. If the g calculated from equation 39 is less than that calculated from equation 40 or 41, the bitumen film strength controls failure.

It is possible to design a single-ply system such that the bitumen and felt layers have equal strength according to the criterion for failure developed in this report. In such a case the bitumen and felt would be predicted to fail at the same joint substrate movement g*. The design thickness of bitumen to use such that bitumen and felt have equal strengths is h*.

For linearly elastic membranes equation 2 can be rearranged to give

$$g^* = \frac{P^2}{M\,\bar{\tau}} \tag{42}$$

or, equivalently

$$h^* = [\frac{P}{\tau}]^2 \frac{G}{M} = \frac{P}{\tau} \frac{\varepsilon_p}{\gamma} \quad (43)$$

The last form (equation 43) is more useful when only ultimate stress data are available. Equation 43 was first presented in a slightly different form by Koike [2] who used it to predict modes of roofing failure. For values of bitumen film thickness less than h*, failure is predicted to occur by bitumen disbonding, while for values greater than h* it is predicted to occur by membrane rupture. Based on Koike's data and methods of obtaining moduli, equation 43 predicts that failure should occur by membrane rupture. Koike found that this was true for all six samples at the higher temperatures (13 and 18°C), but at the lowest temperature (-3°C) he found that bitumen disbonding occurred instead.

Jones [12] applied Koike's theory to some of his own data obtained for a two-ply asphalt-asbestos membrane bonded with asphalt between two adjacent aluminum plates. In all cases the mode of failure agreed with that predicted by equation 43. Thus, with an asphalt thickness of 0.020 in (0.5 mm) Jones found that failure occurred by bitumen disbonding, while with a thickness of 0.042 in (1.1 mm) it occurred by membrane rupture. For each thickness three separate experiments were conducted. Jones obtained moduli M and G in the same way as Koike. The stress-strain curves he obtained for the membrane were distinctly non-linear even at the lowest temperature. No stress-strain curves were given for the bitumen.

For the same system, Jones [12] presents a plot (equation 43) of the critical thickness h* as a function of temperature for two and four-ply membranes in both the machine and cross direction. h* was obtained from the right-hand side of equation 43 using the experimentally determined mechanical properties found at each temperature. Jones found that h* always decreased with increasing temperature, the rate of drop with temperature being greatest for a four-ply membrane in the machine direction and least for a two-ply membrane in the cross direction.

For non-linear membranes, the value of h* can be obtained by substituting equation 39 into equation 38

$$h^* = \frac{M_o \beta^2 [e^{-\alpha\varepsilon_p}(\alpha^2 \varepsilon_p^2 + \alpha\varepsilon_p + 1) - 1]}{G_o \alpha^2 [1 - (\beta \bar{\gamma} + 1) e^{-\beta\bar{\gamma}}]} \tag{44}$$

The corresponding value of g* can be found from equation 39.

Using equation 38 and equation 39, data can be analyzed to determine the incidence and mode of membrane failure for non-linear materials. A convenient way to analyze data is to first write equation 38 in the form

$$1 - (1 + \theta)e^{-\theta} = k\,\theta \tag{45}$$

where

$$\theta = \frac{\beta g}{2h} \tag{46}$$

and

$$k = \frac{2 M_o \beta}{g G_o \alpha^2} [e^{-\alpha\varepsilon_p}(\alpha^2\varepsilon_p^2 + \alpha\varepsilon_p + 1) -1] \tag{47}$$

θ is the dimensionless group defined by equation 46 while k is the constant defined by equation 47.

To evaluate the bitumen film thickness h which is needed to prevent a rupture of the felt for a given gap spacing g, a plot of the left-hand side of equation 45 vs. θ is made. A line of slope k is drawn on this plot and where the line intersects the curve a solution for θ is obtained. Equation 46 can then be solved for the h corresponding to this value of θ.

Figure 7 illustrates the method. Depending on the numerical value of the constant k and the sign of the bitumen strain rate β three kinds of solutions are possible. If β is negative (region A in figure 7) k and θ will be negative, and a single solution is present, denoted by θ_A in figure 7. If β is positive, k and θ will be positive and either two solutions or no solution is present. No solution is present (region B in figure 7) when k is greater than 0.2984, while two solutions are present (region C) when k is less than 0.2984. The value of θ at this value of k is 1.793. The two solutions in region C are denoted as θ_{C1} and θ_{C2} in figure 7.

When no solution is present, this indicates that failure by membrane splitting can not occur at the gap spacing regardless of the value of h. The membrane is strong enough to sustain appreciable substrate movements in region B of figure 7. Further increases in gap spacing g will lower

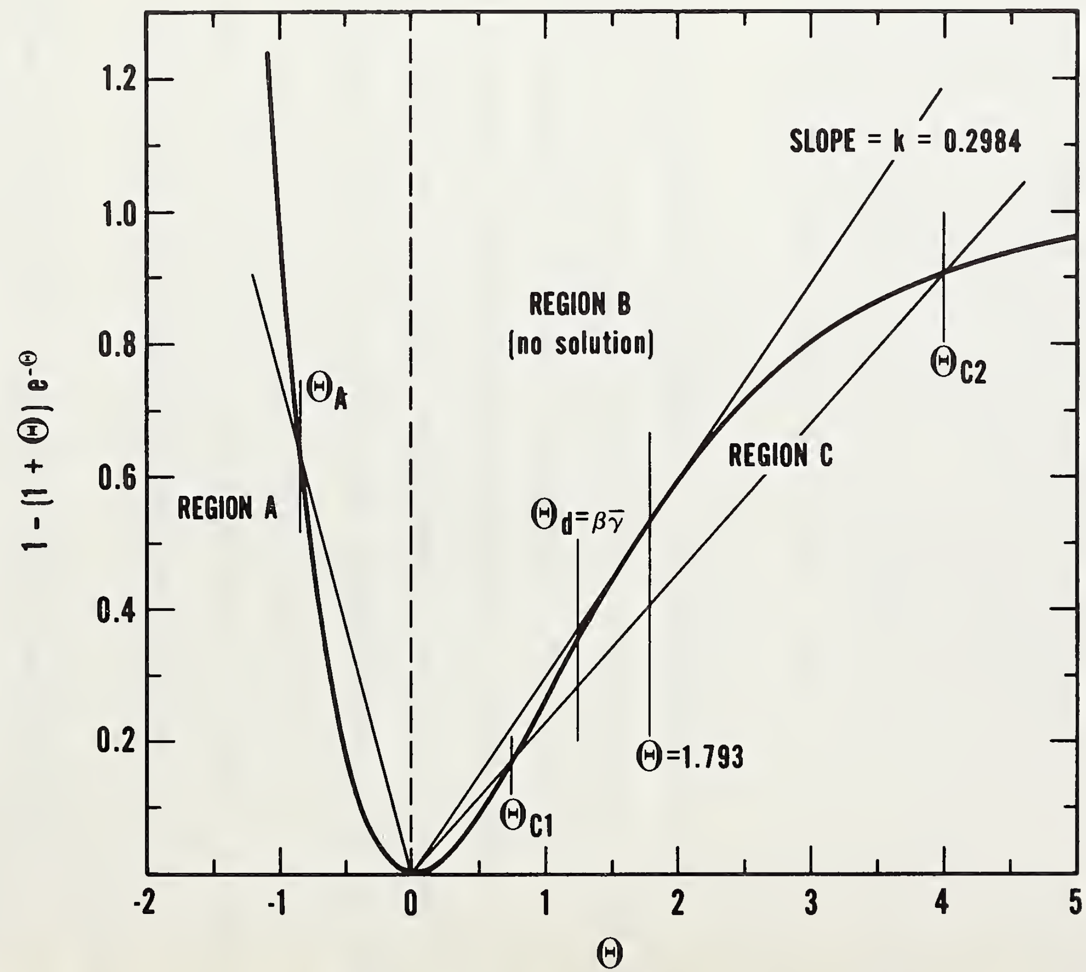

FIGURE 7. REPRESENTATION OF POSSIBLE SOLUTION TYPES (EQUATIONS 45, 46, 47)

the value of k until k = 0.2984, at which failure is predicted if it happens that $h = g\beta/3.586$.

When two solutions are present (region C), this means physically that two different bitumen film thicknesses are capable of sustaining the same substrate movement. Treating this as a design problem, one where h is to be specified, the solution with the smallest value of the film thickness is preferred provided bitumen disbonding does not occur. This will be the one with the largest value of θ (indicated as θ_{C2} on figure 7).

This procedure may also be used to treat the problem of determining at what gap spacing failure by felt rupture will occur for an existing membrane, one whose value of h is fixed. In this case only one solution will be present, one corresponding to either θ_{C1} or θ_{C2} on figure 7, but not both.

Bitumen disbonding will occur if

$$\frac{g}{2h} = \frac{\theta}{\beta} > \bar{\gamma} \tag{48}$$

Viewing this as a design problem, the larger value of h should be chosen in hopes that the yield strain $\bar{\gamma}$ of the bitumen will not be exceeded, so that the bitumen is capable of sustaining more lateral movement before disbonding.

Figure 7 shows how the selection of the mode of failure can be quantified. A vertical line is drawn at an illustrating value of $\theta_d = \beta\bar{\gamma}$, where θ_d is the value corresponding to incipient failure by bitumen disbonding. If the roofing membrane is designed for equal strength felt and bitumen layers, then $\theta = \theta_d$. The value of the bitumen film thickness to use in this case is h* as given by equation 44. Since these correspond to small values of θ, the smallest value of θ is preferred (θ_{C1} in figure 7). For an existing membrane, the value of θ calculated from equation 46 will either be larger or smaller than θ_d. If $\theta < \theta_d$, then failure by felt rupture is predicted, whereas if $\theta > \theta_d$, then failure by bitumen disbonding should occur.

Table 3 presents the major results of the present study. At temperatures of -3°C, 13°C, and 18°C, and three different bitumen thicknesses, the experimental results of Koike [2] for the substrate joint movement needed to cause felt rupture are compared with the theoretical predictions for both linear and non-linear membrane materials. Experimental results at -3°C were not available for comparison with the theoretical predictions since bitumen disbonding occurred [2].

Also given in table 3 are the joint movements which are needed to cause bitumen disbonding (third column from the right in table 3). The last two columns in table 3 present the joint movements g* and film thicknesses h* at which the bitumen and felt would have equal strengths, that is, the condition under which failure by bitumen disbonding and felt rupture would be equally probable.

For linearly elastic membranes the theoretical predictions of substrate joint movement g (fourth column from the left in table 3) were obtained in the same manner as that employed by Koike [2], that is, by an application of equation 2. His value for the modulus M was equal to the physically measured initial slope of the stress-strain diagram of the roofing felt, while he took G equal to the slope of a line drawn

Table 3. Comparison of Test Results for Joint Movements [2] with Theory

Temp. °C	Film Thickness h mm	Test [2]	Calculated Substrate Joint Movement g: of Felt Linear	of Felt-Linear Half-Height	of Felt Non-Linear	of Bitumen	Equal Strength Joint Movements g*, and Film Thicknesses h* Theoretical Predictions	
			g 1/ mm	g 2/ mm	g 3/ mm	g 4/ mm	g* 5/ mm	h* 6/ mm
	1.5	7/	0.86	1.14	1.27	1.44		
-3 9/	2.0	7/	1.00	1.32	1.51	1.92	1.05	1.10
(-2)	2.5	7/	1.11	1.48	1.73	2.40	(1.04) 8/	(1.08) 8/
	1.5	1.0	0.81	1.03	1.11	1.57		
13	2.0	0.9	0.94	1.19	1.30	2.10	0.71	0.68
(10)	2.5	1.0	1.05	1.34	1.46	2.62	(1.23)	(1.17)
	2.0	1.0	1.15	1.21	1.24	1.98		
18	2.5	1.4	1.29	1.35	1.38	2.48	0.81	0.82
(20)	3.0	1.7	1.42	1.48	1.50	2.98	(1.71)	(1.72)

1/ Calculated using previous theory for linear materials equation 2, based on data of Koike [2] and equations 9 and 10.
2/ Calculated using equation 2 with half-height method (refer to p. 48) to obtain moduli M and G.
3/ Results for present theory for non-linear materials, calculated from equation 38.
4/ Joint movement needed to disbond bitumen from substrate, calculated from equation 39.
5/ Results for the present theory for non-linear materials, calculated from equation 39.
6/ Results for the present theory for non-linear materials, calculated from equation 44.
7/ Bonding bitumen was separated from the surface of the substrate, without rupture of the felt [2].
8/ Results in parentheses in these columns are for linear materials, calculated using equations 42 and 43.
9/ Felt temperatures [2], bitumen temperatures in parentheses.

from the origin of the stress-strain diagram of the bitumen out to the ultimate or breaking stress of the bitumen. In this report the corresponding value of M is M_o in equation 13, and G is the ratio of the bitumen breaking stress to the strain at that point. The values for g calculated by this procedure do not differ substantially from those reported by Koike [2].

Koike's method of obtaining the moduli M and G is somewhat arbitrary since the procedure could be reversed to obtain G from an initial slope, and M as the ratio of coordinates at the yield point. Employing this procedure gives a significantly different set of results for predicted joint movements than if M is obtained from an initial slope and G as the ratio of coordinates at the ultimate stress. For consistency it would have been better to define both moduli at the same point, either at zero stress or at the ultimate stress or at some well-defined halfway point. Koike [2] did not give a reason for his choice of method.

Table 3 shows a wide variation in predicted joint movements depending on what model is used to calculate them. For the non-linear model of the present study the predicted value of the joint movement g rises with the value of the bitumen film thickness h. According to the linear theory (equation 2), the joint spacing for a given linearly elastic membrane should rise in proportion to the square root of the film thickness. For membrane materials with non-linear stress-strain behavior this was found at 13°C, but at -3°C the predicted gap spacing increased more rapidly than that predicted by the linear theory while at 18°C it increased more slowly.

Table 3 shows that as the temperature falls the substrate is able to sustain more movement. This is a consequence of the greater complementary strain energies of the felt at the lower temperatures. Predictions of the non-linear theory gave permissible substrate movements which were 5% higher at 13°C than at 18°C and over 20% higher at -3°C than at 18°C.

Koike [2] found that bitumen disbonding was the mode of membrane failure at -3°C. This result is not consistent with prediction. Table 3 presents a column (third from the right) which gives the predicted substrate joint movement needed to cause failure by bitumen disbonding. These values were calculated from equation 39. In all cases the joint movements calculated exceeded the experimental values and those predicted from the linear and non-linear theories. This indicates that the bitumen film should be stronger than for the roofing felt, but such was evidently not the case at -3°C. Koike [2] attributes this anomalous result to a difference in experimental technique.

Note from table 3 that failure by bitumen disbonding is more likely at lower temperatures where g values for bitumen and felt are closer. At some temperature even lower than -3°C the g values for bitumen and felt might become equal in which case failure by either bitumen disbonding or felt rupture would be equally likely. In this event the felt and bitumen can be considered to have equal strengths.

The last two columns in table 3 summarize for each temperature the predicted values of joint spacing (g*) and bitumen film thickness (h*) which would be needed to give equal strengths of bitumen and felt layers. These were calculated using equations 39 and 44, respectively.

Also included in parenthesis below each value are the corresponding values calculated using equations 42 and 43 for membrane materials with linear stress-strain response. At -3°C values of g* and h* are equivalent (1 mm) regardless of whether the membrane had linear or non-linear stress-strain characteristics. At higher temperatures the values of g* and h* are about twice as high for membranes with linear behavior as for membrane materials with non-linear behavior. As pointed out in the last section, g* and h* are useful for membrane design. At the higher temperatures, gap widths or spacings are greater than predicted for membranes with linear stress-strain behavior. In practice an actual membrane would not sustain nearly as much substrate movement before failure.

To quantify the differences between the different methods or models for predicting substrate joint movements equation 49 is used

$$s^2 = \sum_{i=1}^{n} \frac{(g_{ti}-g_{ei})^2}{n-1} \tag{49}$$

s^2 represents the sample variance of the difference between the theoretical (g_{ti}) and experimental (g_{ei}) values of the joint width. n denotes the number of data points at each temperature (three here). Relatively low values of the sample variance indicate good agreement between experimental and predicted values.

Table 4 summarizes the results of the calculations. Each of the linear models are characterized in terms of the assumptions made to obtain their moduli from the stress-strain diagrams for the roofing felts and roofing bitumens (second column of table 4). In the third

Table 4. Statistical Results for Methods used to Predict Substrate Joint Movements needed for Felt Rupture (data from [2])

Model Linearity	Assumptions Made to Obtain Moduli from Stress-Strain Diagrams	Variance of Joint Movement[2], mm^2 (Theoretical-Experimental)[1]		Variance Ratio[3]	
		13°C	18°C	13°C	18°C
Non-Linear[3]	none	0.19	0.05	1.0	1.0
Linear[4]	M zero-stress slope,[5] G from ultimate stress coordinate ratio	0.02	0.06	0.1	1.2
Linear[4]	G from zero-stress slope, M from ultimate stress coordinate ratio	1.91	0.30	9.5	6.0
Linear[4]	M and G from zero-stress slopes	0.12	0.14	0.6	2.8
Linear[4]	M and G from ultimate stress coordinate ratios	0.64	0.72	3.3	14.4
Linear[4]	M and G from coordinate ratio of point at half the ultimate stress (half-height method)	0.10	0.05	0.5	1.0

1/ Defined and calculated from equation 49.
2/ Ratio of variances of joint movements relative to the non-linear model at the same temperature.
3/ Results for present theory for non-linear materials (equation 38).
4/ Results for previous theory for linear materials (equation 2).
5/ Method used by Koike [2] in his data analysis.

column of the table variances between the theoretical and experimental joint widths calculated using equation 49 are presented. Examining table 4 shows a wide range in variances calculated from equation 49 depending upon the convention adopted for choosing the moduli. For roofing materials with non-linear stress-strain characteristics, no assumptions are involved so that this forms a convenient basis for comparison. The last column gives the ratio of the variance of the linear model to that of the non-linear model. Variance ratios are generally greater than unity, indicating that the non-linear model usually gives a closer fit to the experimental results, especially at the higher temperature (18°C).

Comparing the variances of the linear to the non-linear model, only the linear model of Koike [2] (second row in table 4) and that based on the values of M and G obtained from the coordinate ratio of the point at half the ultimate stress (last row in table 4), called the half-ultimate stress point,[1/] gave better results than the non-linear model. This latter model works well because it partially accounts for the non-linearities in the stress-strain curves. The method of drawing a line from the origin through a point on the stress-strain curve located at half the ultimate stress (last row in table 4) tends to give strain energies equal to the non-linear values. This is because, for the stress-strain data used in this study, the line subtends and excludes about equal areas when drawn with the stress-strain curve, and by the mean value theorem of calculus, approximately equal strain energies

[1/] Denoted as the half-height method.

result. In systems where non-linearities are more pronounced this may not be the case.

All of the models examined (refer to table 4) involve assumptions about the choice of moduli except for the non-linear model. The non-linear model is more general since it reduces to the linear models for roofing materials which have linear stress-strain characteristics. As discussed, the convention adopted for choosing the moduli for the linear models is arbitrary, and, in fact, there is no theoretical basis for adopting one linear model compared to another. In addition, it would seem to be more consistent to define the moduli M and G in a similar fashion either as the zero-stress slopes of their respective stress-strain diagrams (4th row in table 4) or as the ultimate stress coordinate ratios (5th row in table 4). However, these models generally give larger variance ratios when compared to the non-linear model, especially at the higher temperature.

In general, the non-linear model is preferred because it is exact and does not depend on any assumptions about the moduli. However, in some specific cases, it may be preferable for estimation purposes to use a simpler procedure such as the half-height method (last row in table 4) which may account satisfactorily for non-linearities. If such a procedure is used it is recommended that it should be checked, where stress-strain data for roofing materials are available, against the criterion for failure (equation 36 or 38) developed in this report.

5. SUMMARY AND CONCLUSIONS

Rupture of built-up roofing membranes resulting from movements of the underlying deck or substrate is an important cause for water leakages in roofs. Similarly, bitumen or adhesive disbonding without membrane rupture is a potential cause of the formation of roof blisters, which themselves often lead to water penetration and subsequent rupture.

This report develops and applies visco-elastic theory to the calculation of membrane and adhesive stresses and strains in a single-ply fabric or felt, which, except at the joints between adjacent substrate sections, is fully bonded to the substrate with a layer of adhesive or bitumen. The theory applies to fabric and adhesive layers with both linear and non-linear stress-strain behavior. For materials with linear stress-strain characteristics it is shown that the theory reduces to previously published work.

A method was developed for accurately fitting non-linear stress-strain data for roofing materials to a constitutive equation having only two adjustable constants. The method was applied to stress-strain roofing felt and roofing bitumen data from the literature [2] obtained at three different temperatures. The constitutive equation was shown to reduce to Hooke's law for linearly elastic materials at low values of stress.

The joint width between substrate sections, the bitumen layer thickness, and the mechanical properties of the felt and bitumen, were important parameters in the mathematical models developed, while the dimensions of the substrate section were not.

A criterion for failure indicating either rupture of the felt or disbonding of the bitumen was established. Specifically, it was found that failure was predicted when the product of the strain energy of the bitumen with the bitumen thickness was equal to the complementary strain energy of the felt. The highest strain energy that either material can accommodate was one corresponding to its ultimate stress. In accord with the criterion, whenever the lower of these two energies was reached, failure was predicted in that mode.

The theory developed for the mechanical performance of roofing membranes was applied at three different temperatures to non-linear stress-strain data obtained for roofing felts and bitumens bonded to a concrete deck [2]. Predicted results agreed well with the theory. Also, as predicted by the failure criterion, at temperatures of 18°C and 13°C failure occurred by membrane rupture. At -3°C it occurred by bitumen disbonding, although the theory also predicted failure by membrane rupture.

Based on the criterion for failure, an equation was developed which predicted the bitumen interply thickness at which the adhesive and fabric (bitumen and felt) were equally likely to fail. Substrate movements necessary to produce failure were presented as a function of system parameters.

For the best mechanical strength, it is recommended that, within other constraints, roofing membranes be selected or designed which have strain energies and interply thicknesses compatible with one another according to the criterion for failure.

6. REFERENCES

1. Bonafont, R. L., "Research into Mechanical Behaviour of Waterproofing Membrane Systems," International Symposium on Roofs and Roofing, (Paper No. 9), Brighton, England, September 1974.

2. Koike, M., "Elastic Analysis of Ruptures of Bitumen-Felt Roof Coverings Caused by Cracks in Substructures," BRI Occasional Report (No. 15), Building Research Institute of Japan, December 1963.

3. Cullen, W. C. and Boone, T. H., "Thermal-shock resistance for built-up membranes," National Bureau of Standards, Building Science Series 9, August 1967.

4. Cullen, W. C., "Solar Heating, Radiative Cooling, and Thermal Movement-Their Effects on Built-up Roofing," National Bureau of Standards (U.S.) Technical Note 231, December 1963.

5. Marijs, P. D. and Bonafont, R. L., "Mechanical Behaviour of Bituminous Waterproofing Membrane Systems," J. Appl. Chem., 20, pp. 11-20, 1970.

6. Mathey, R. G. and Cullen, W. C., "Preliminary Performance Criteria for Bituminous Membrane Roofing," National Bureau of Standards, Building Science Series 55, November 1974.

7. Rossiter, W. J., Jr. and Mathey, R. G., "Effect of Insulation on the Surface Temperature of Roof Membranes," National Bureau of Standards (U.S.) NBSIR 76-987, February 1976.

8. Bonafont, R. L., "Application of Performance Concept in Evaluation, Specification, and Selection of Roofing Materials," Proceedings of the Symposium on Roofing Technology, (Paper No. 11) pp. 70-85, National Bureau of Standards, Washington, D.C., September 1977.

9. Koike, M., Tanaka, K. and Tomiita, T., "Strains in Multi-ply Membranes Caused by Joint Movement in Substrate," Report of the Research Laboratory of Engineering Materials (Number 3), Tokyo Institute of Technology, 1978.

10. Heukelom, W., "Observations on the Rheology and Fracture of Bitumens and Asphalt Mixes," Shell Bitumen Reprint No. 19, Shell International Petroleum Company Limited, London, 1966.

11. Timoshenko, S. P. and Gere, J. M., Mechanics of Materials, Chapter 11, Van Nostrand-Reinhold Co., New York, 1972.

12. Jones, P. M., "Load-Strain Properties and Splitting of Roof Membranes," Engineering Properties of Roofing Systems, ASTM STP409, Am. Soc. Testing Mats., 1967.

7. NOMENCLATURE

a	parameter in equation 3, defined by equation 4, mm^{-1}
B	width of the membrane, mm
C_1	integration constant, equation 34
g	joint substrate movement (half the gap spacing), mm
g^*	joint substrate movement for equal strengths of bitumen and felt, mm
G	shear modulus of bitumen (adhesive) film, N/mm^2
G_o	shear modulus of bitumen film at zero stress, N/mm^2
h	thickness of bitumen (adhesive) film, mm
h^*	bitumen film thickness for equal strengths of bitumen and felt, mm
i	index of summation, equation 49
g_{ei}	experimental value of g, mm
g_{ti}	theoretical (predicted) value of g, mm
k	constant defined by equation 47
M	elastic modulus of membrane or felt (fabric), N/mm
M_o	elastic modulus of felt at zero stress, N/mm
n	number of data points, equation 49
N	number of plies in a built-up roofing membrane
P	tensile strength, ultimate or breaking load (force/unit width) of membrane or roofing felt, N/mm
r	correlation coefficient
s	sample standard deviation
s_α	sample standard deviation on α
s_β	sample standard deviation on β
s_r	sample residual standard deviation
s_{G_o}	sample standard deviation on G_o

s_{M_o} sample standard deviation on M_o

s^2 sample variance, equation 49

t student's t

TSF thermal shock factor, defined by equation 1

u membrane displacement, mm

U complementary strain energy of the felt, equation 28

v substrate displacement, mm

V volume of membrane system, mm^3

W half-width of one substrate element, mm

x membrane displacement measured from the center of the gap, mm

α felt constant, equation 13; coefficient of linear thermal expansion, equation 1

β bitumen or adhesive constant, equation 16

γ bitumen or adhesive strain, equation 22

$\bar{\gamma}$ bitumen strain corresponding to $\bar{\tau}$

ε felt or fabric strain, equation 20

ε_m felt strain at maximum stress

ε_p felt strain at ultimate stress P

ζ substrate strain, equation 21

θ dimensionless group, defined by equation 46

σ felt or fabric stress (N/mm^2)

σ_m maximum stress, calculated from $0.368\ M_o/\alpha$, N/mm^2

τ bitumen or adhesive stress, N/mm^2

$\bar{\tau}$ bitumen film yield strength, N/mm^2

NBS-114A (REV. 2-80)

U.S. DEPT. OF COMM. **BIBLIOGRAPHIC DATA SHEET** *(See instructions)*	1. PUBLICATION OR REPORT NO. TN 1152	2. Performing Organ. Report No.	3. Publication Date December 1981

4. TITLE AND SUBTITLE

Mechanical Performance of Built-Up Roofing Membranes

5. AUTHOR(S)

James M. Pommersheim and Robert G. Mathey

6. PERFORMING ORGANIZATION *(If joint or other than NBS, see instructions)*

NATIONAL BUREAU OF STANDARDS
DEPARTMENT OF COMMERCE
WASHINGTON, D.C. 20234

7. Contract/Grant No.

8. Type of Report & Period Covered

Final

9. SPONSORING ORGANIZATION NAME AND COMPLETE ADDRESS *(Street, City, State, ZIP)*

Same as no. 6

10. SUPPLEMENTARY NOTES

☐ Document describes a computer program; SF-185, FIPS Software Summary, is attached.

11. ABSTRACT *(A 200-word or less factual summary of most significant information. If document includes a significant bibliography or literature survey, mention it here)*

For built-up roofing membranes with either linear or non-linear stress-strain behavior, fully bonded to an underlying deck or substrate which undergoes displacement, it is the equality of the complementary strain energy of the fabric or felt layer with the strain energy of the bonding adhesive or bitumen layer, which governs both the conditions under which membrane integrity is lost and the mode of failure by either membrane splitting or adhesive bonding. The testing criteria developed are applied to a sample case.

12. KEY WORDS *(Six to twelve entries; alphabetical order; capitalize only proper names; and separate key words by semicolons)*

adhesive; bitumen; bonding; built-up roofing membrane; complementary strain energy; felt; non-linear; roofing membrane; splitting; strain energy; stress; substrate.

13. AVAILABILITY

☐ Unlimited
☐ For Official Distribution. Do Not Release to NTIS
☐ Order From Superintendent of Documents, U.S. Government Printing Office, Washington, D C 20402.
☒ Order From National Technical Information Service (NTIS), Springfield, VA. 22161

14. NO. OF PRINTED PAGES

60

15. Price

USCOMM-DC 6043-P80

NBS TECHNICAL PUBLICATIONS

PERIODICALS

JOURNAL OF RESEARCH—The Journal of Research of the National Bureau of Standards reports NBS research and development in those disciplines of the physical and engineering sciences in which the Bureau is active. These include physics, chemistry, engineering, mathematics, and computer sciences. Papers cover a broad range of subjects, with major emphasis on measurement methodology and the basic technology underlying standardization. Also included from time to time are survey articles on topics closely related to the Bureau's technical and scientific programs. As a special service to subscribers each issue contains complete citations to all recent Bureau publications in both NBS and non-NBS media. Issued six times a year. Annual subscription: domestic $13; foreign $16.25. Single copy, $3 domestic; $3.75 foreign.

NOTE: The Journal was formerly published in two sections: Section A "Physics and Chemistry" and Section B "Mathematical Sciences."

DIMENSIONS/NBS—This monthly magazine is published to inform scientists, engineers, business and industry leaders, teachers, students, and consumers of the latest advances in science and technology, with primary emphasis on work at NBS. The magazine highlights and reviews such issues as energy research, fire protection, building technology, metric conversion, pollution abatement, health and safety, and consumer product performance. In addition, it reports the results of Bureau programs in measurement standards and techniques, properties of matter and materials, engineering standards and services, instrumentation, and automatic data processing. Annual subscription: domestic $11; foreign $13.75.

NONPERIODICALS

Monographs—Major contributions to the technical literature on various subjects related to the Bureau's scientific and technical activities.

Handbooks—Recommended codes of engineering and industrial practice (including safety codes) developed in cooperation with interested industries, professional organizations, and regulatory bodies.

Special Publications—Include proceedings of conferences sponsored by NBS, NBS annual reports, and other special publications appropriate to this grouping such as wall charts, pocket cards, and bibliographies.

Applied Mathematics Series—Mathematical tables, manuals, and studies of special interest to physicists, engineers, chemists, biologists, mathematicians, computer programmers, and others engaged in scientific and technical work.

National Standard Reference Data Series—Provides quantitative data on the physical and chemical properties of materials, compiled from the world's literature and critically evaluated. Developed under a worldwide program coordinated by NBS under the authority of the National Standard Data Act (Public Law 90-396).

NOTE: The principal publication outlet for the foregoing data is the Journal of Physical and Chemical Reference Data (JPCRD) published quarterly for NBS by the American Chemical Society (ACS) and the American Institute of Physics (AIP). Subscriptions, reprints, and supplements available from ACS, 1155 Sixteenth St., NW, Washington, DC 20056.

Building Science Series—Disseminates technical information developed at the Bureau on building materials, components, systems, and whole structures. The series presents research results, test methods, and performance criteria related to the structural and environmental functions and the durability and safety characteristics of building elements and systems.

Technical Notes—Studies or reports which are complete in themselves but restrictive in their treatment of a subject. Analogous to monographs but not so comprehensive in scope or definitive in treatment of the subject area. Often serve as a vehicle for final reports of work performed at NBS under the sponsorship of other government agencies.

Voluntary Product Standards—Developed under procedures published by the Department of Commerce in Part 10, Title 15, of the Code of Federal Regulations. The standards establish nationally recognized requirements for products, and provide all concerned interests with a basis for common understanding of the characteristics of the products. NBS administers this program as a supplement to the activities of the private sector standardizing organizations.

Consumer Information Series—Practical information, based on NBS research and experience, covering areas of interest to the consumer. Easily understandable language and illustrations provide useful background knowledge for shopping in today's technological marketplace.

Order the **above** *NBS publications from: Superintendent of Documents, Government Printing Office, Washington, DC 20402.*

Order the **following** *NBS publications—FIPS and NBSIR's—from the National Technical Information Services, Springfield, VA 22161.*

Federal Information Processing Standards Publications (FIPS PUB)—Publications in this series collectively constitute the Federal Information Processing Standards Register. The Register serves as the official source of information in the Federal Government regarding standards issued by NBS pursuant to the Federal Property and Administrative Services Act of 1949 as amended, Public Law 89-306 (79 Stat. 1127), and as implemented by Executive Order 11717 (38 FR 12315, dated May 11, 1973) and Part 6 of Title 15 CFR (Code of Federal Regulations).

NBS Interagency Reports (NBSIR)—A special series of interim or final reports on work performed by NBS for outside sponsors (both government and non-government). In general, initial distribution is handled by the sponsor; public distribution is by the National Technical Information Services, Springfield, VA 22161, in paper copy or microfiche form.

U.S. DEPARTMENT OF COMMERCE
National Bureau of Standards
Washington, DC 20234

OFFICIAL BUSINESS

Penalty for Private Use, $300

POSTAGE AND FEES PAID
U.S. DEPARTMENT OF COMMERCE
COM—215

U.S.MAIL

THIRD CLASS